

# The Synthesis of Vanadium-Doped Forsterite by the H<sub>2</sub>O<sub>2</sub>-Assisted Sol-Gel Method, and the Growth of Single Crystals of Vanadium-Doped Forsterite by the Floating Zone Method

Dong Gon Park\*, Mikio Higuchi<sup>†</sup>, Rüdiger Dieckmann<sup>‡</sup>, and James M. Burlitch<sup>‡</sup>

Department of Chemistry, Sookmyung Women's University, Seoul 140-742, Korea

<sup>†</sup>Division of Materials Science and Engineering, Hokkaido University, Hokkaido, Japan

<sup>‡</sup>Department of Materials Science and Engineering, Cornell University, Ithaca, NY 14850, USA

<sup>‡</sup>Department of Chemistry, Cornell University, Ithaca, NY 14750, USA

Received February 19, 1998

Polycrystalline powder of vanadium-doped forsterite (V<sub>δ</sub>Mg<sub>2</sub>SiO<sub>4</sub>) was synthesized by the H<sub>2</sub>O<sub>2</sub>-assisted sol-gel method. The vanadium dopant, which was added as VO(OMe)<sub>3</sub> in methanol, went through several redox reactions as the sol-gel reaction proceeded. Upon adding VO(OMe)<sub>3</sub> to a mixture of Mg(OMe)<sub>2</sub> and Si(OEt)<sub>4</sub> in methanol, V(V) reduced to V(IV). As hydrolysis reaction proceeded, the V(IV) oxidized all back to V(V). Apparently, some of the V(V) reduced to V(IV) during subsequent gelation by condensation reaction. The V(IV) remained even after heat treatment of the gel in highly oxidizing atmosphere. The crystallization of the xerogel around 880 °C readily produced single phase forsterite without any minor phase. Using the polycrystalline powder as feeding stock, single crystals of vanadium-doped forsterite were grown by the floating zone method in oxidizing or reducing atmosphere. The doping was limited in low level because of the high partitioning of the vanadium in liquid phase during melting. The greenish single crystal absorbed visible light of 700~1100 nm. But, no emission was obtained in near infrared range.

## Introduction

Forsterite (Mg<sub>2</sub>SiO<sub>4</sub>) is one of very common minerals, which belongs to olivine family, (Mg,Fe)<sub>2</sub>SiO<sub>4</sub>, of orthosilicates.<sup>1</sup> Being a major component of the upper mantle of the Earth, extensive study on its properties has been carried out mostly on geological incentives.

Recently, the single crystal of forsterite was reported to produce widely tunable laser in technologically attractive near infrared range of ~1.1 to ~1.4 μm, when doped with chromium.<sup>2</sup> Since the color center of the laser was reported to be chromium in its higher oxidation state of VI<sup>3</sup> (it used to be III as in Ruby,<sup>4</sup> or in chromium-doped alexandrite<sup>5</sup>), there was a continuing effort to grow single crystals of chromium-doped forsterite in highly oxidizing atmosphere.

Because of several practical reasons such as high melting temperature of forsterite (~2000 °C) and facile oxidation of iridium crucible, which is only available crucible for high melting forsterite, single crystals of chromium-doped forsterite with practical size grown in highly oxidizing atmosphere had been unattainable, until it was first grown by the floating zone method in pure oxygen at 2-3 atm pressure.<sup>6</sup> A crucial factor to the successful preparation of chromium-doped forsterite in highly oxidizing atmosphere by the floating zone method was to use single phase polycrystalline powder of chromium-doped forsterite as a feeding stock.

The powder was synthesized *via* the H<sub>2</sub>O<sub>2</sub>-assisted sol-gel method. High degree of homogeneity attained during the H<sub>2</sub>O<sub>2</sub>-assisted sol-gel method facilitated the synthesis of single phase forsterite powder at ease, without any formation of enstatite (MgSiO<sub>3</sub>) minor phase (a major cause of the multi-phase formation). The crystallization process of the xerogel

precursor was probed by FTIR, magic angle spinning solid state <sup>29</sup>Si NMR, thermal analyses<sup>7</sup> and by in-situ high temperature X-ray diffraction.<sup>8</sup> Solution intermediates that formed during the synthesis were characterized by GLC analysis of the head space,<sup>9</sup> and by <sup>29</sup>Si and <sup>25</sup>Mg NMR spectroscopy.<sup>10</sup> Because of the attainment of the homogeneity, this method is very useful in doping known amount of dopant ions without any introduction of unintended impurities.

Once single crystals of chromium-doped forsterite were synthesized in highly oxidizing atmosphere, we tried to obtain single crystals of forsterite doped with other dopant ions. In this study, we report the synthesis of single phase polycrystalline powder of vanadium-doped forsterite by the H<sub>2</sub>O<sub>2</sub>-assisted sol-gel method, and the growth of the single crystals of vanadium-doped forsterite by the floating zone method using the powder as a feedstock.

## Experimentals

Magnesium in a form of turnings, 99.95%, was obtained from Aldrich. Tetraethylorthosilicate (TEOS), 99+%, and vanadium oxychloride (VOCl<sub>3</sub>), 99%, were used as received from Aldrich. All other chemicals were reagent grade.

Powder X-ray diffraction (PXRD) patterns were taken with a Scintag PAD X diffractometer. Electron spin resonance (ESR) spectra were taken with a Bruker ER 200 D-SRC spectrometer in 9.6 GHz. Simultaneous thermogravimetric/differential thermal analysis (TG/DTA) was carried out on a Seiko TG/DTA-320 instrument. Elemental analyses were done by induced coupled plasma/mass spectrometry (ICP/MS) and microprobe analysis (WDS). Absorption spectra from the single crystals were measured by Varian Cary-5 UV-vis-NIR spectrophotometer. A Nd:YAG laser was used to excite the single crystal, and a scanning monochromator

\*Author to whom correspondence should be addressed.

measured the resulting fluorescence spectra.

#### Xerogel precursors to vanadium-doped forsterite.

All procedures that involved solution were carried out under a dry and oxygen-free argon atmosphere.<sup>11</sup> Methanol was degassed and distilled over  $\text{Mg}(\text{OMe})_2$ . Vanadium was doped as vanadium oxotrimethoxide ( $\text{VO}(\text{OMe})_3$ ) prepared from vanadium oxotrichloride.<sup>12</sup> Magnesium, 4.70 g (0.193 mole), was charged into a 1-L 3-necked round bottom flask equipped with a water-cooled condenser, which was connected to a source of argon via a 3-way stopcock. Via cannula, 500 mL of dried MeOH was transferred onto the magnesium. After all the magnesium reacted with MeOH, the solution was filtered through fritted filter tube, into a dry 2-L round bottom creased flask, equipped with a water condenser and a mechanical stirrer with a Teflon paddle. The 1-L flask and the filter tube were rinsed with 50 mL of MeOH. TEOS (20.1 g, 0.0964 mol), weighed in a 50 mL Schlenk reaction vessel (SRV), was combined with the  $\text{Mg}(\text{OMe})_2$  solution in the 2-L creased flask via a cannula, and the SRV was rinsed with 50 mL of MeOH. All the rinsings were added to the reaction mixture.  $\text{VO}(\text{OMe})_3$  ( $9.7 \times 10^{-4}$  mol) was added on the reaction mixture and was well mixed. The reaction mixture was hydrolyzed by dropwise addition of 10.3 g of 30%  $\text{H}_2\text{O}_2$  in 200 mL of MeOH, during 17 h with vigorous stirring. The partially hydrolyzed sol was further hydrolyzed by the dropwise addition of 3.5 g of  $\text{H}_2\text{O}$  in 200 mL of MeOH during 17 h. The sol with light yellow tint was heated at reflux for 6 h, after which the sol became slightly hazy. The solvent was removed from the sol by rotary evaporation by steam-heating under reduced pressure. The resulting grains of xerogel was reduce to a fine pale yellow powder by grinding with an agate mortar and pestle. Polycrystalline powder was obtained by heating the xerogel at 1000-1100 °C for 2-4 h, in water-saturated oxygen or in a gas mixture of CO,  $\text{CO}_2$ , and Ar (1 : 5 : 10 volume ratio).

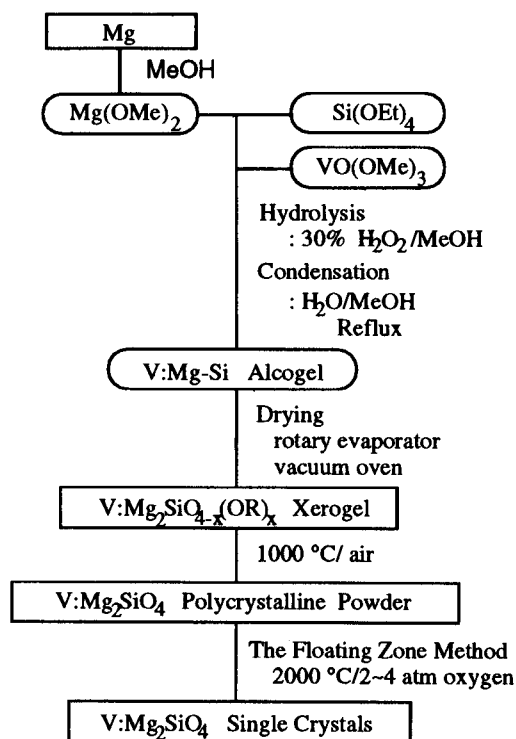
#### Single crystal growth by the floating zone method.

Single crystals of vanadium-doped forsterite were grown by the floating zone method.<sup>13</sup> Not like the chromium-doped forsterite single crystals grown and reported in previous study,<sup>6</sup> the single crystals in this study were grown by applying double melting technique,<sup>14</sup> to remove any possible source of bubbles and to get homogeneous dopant concentration throughout the crystal. The polycrystalline powders were cold-pressed into 10 mm diameter 40 mm long cylindrical rods, and were sintered at 1200 °C for 3 h in ambient air. Unlike in conventional method, no binder or sintering aid was used. In ellipsoid mirror furnace, these feeding rods were melted (first melting) by focused beam at ~1900 °C in argon atmosphere at fairly fast pulling rate of 20 mm/h. This first melting eliminated bubbles originated from porosity that is intrinsically present in the products via sol-gel method. In second melting, the large grained polycrystalline rods gotten from the first melting were used as feeding rods. Pulling rate during this second melting was 2 mm/h. Single crystals of vanadium-doped forsterite were grown both in highly oxidizing atmosphere of pure oxygen, or in reducing atmosphere (the mixture of CO,  $\text{CO}_2$ , and Ar). The single crystals of vanadium-doped forsterite in rod shape were oriented by real time Laue backscattering technique, and cut into several pieces of roughly cubic shaped single crystals for spectroscopy.

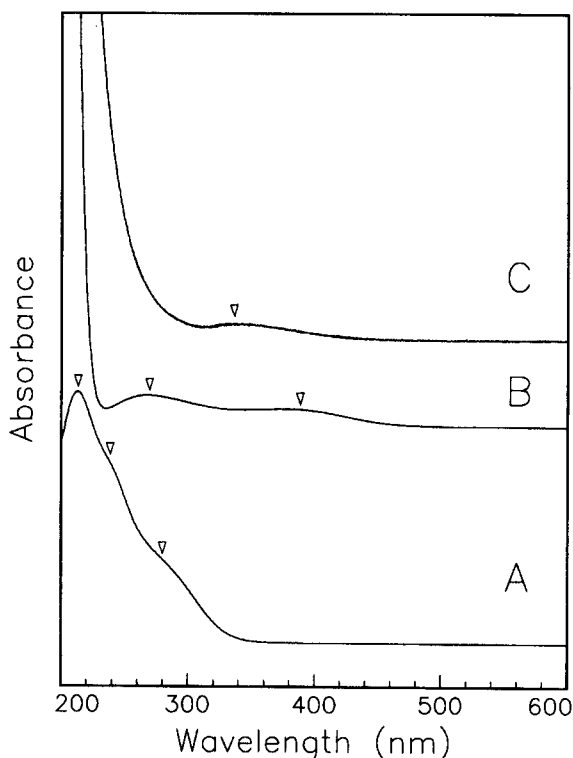
## Results and Discussion

Figure 1 shows overall scheme of the syntheses of vanadium-doped forsterite. Main effort in preparing the xerogel was to eliminate any formation of precipitates to keep the homogeneity of the precursor throughout the synthesis, to minimize solid state diffusion barrier that would prevent crystallization of the precursor into single phase forsterite at low temperature. Unlike in a simple system with a single metal component, such as in silica or alumina, any formation of precipitates will introduce stoichiometric inhomogeneity, because the number of metal components was more than one. The high degree of homogeneity was accomplished by discouraging the formation of any precipitates that would be visible as cloudiness of the sol, by using  $\text{H}_2\text{O}_2$  as catalyst<sup>6</sup> instead of acid or base, by diluting all the reactants and hydrolyzing reagents prior to mixing, and by adding the hydrolyzing reagents ( $\text{H}_2\text{O}_2$  and  $\text{H}_2\text{O}$ ) very slowly with vigorous stirring. The sol was clear after all the hydrolyzing agents were added, indicative of the homogeneity.<sup>7</sup> Monoliths prepared by slowly drying the gel were also clear.

The synthesis of the vanadium-doped gel was followed by UV-vis and ESR spectroscopy (Figure 2, 3, 4, and 5). There were contradictory reports on the oxidation state of vanadium in crystalline  $\text{VO}(\text{OMe})_3$ , which had been described as vanadium (IV) or vanadium (V).<sup>15</sup> The spectrum of bluish green solution of  $\text{VO}(\text{OMe})_3$  in methanol (Figure 2a) had three peaks at 213 (s), 240 (sh), and 280 nm (sh). No ESR signal was observed from the solution. Therefore, the oxidation state of vanadium of  $\text{VO}(\text{OMe})_3$  in methanol solution should be V. The spectrum resembled that of  $\text{VO}(\text{acac})_2$ ,<sup>16</sup> whose



**Figure 1.** Schematic outline of the preparation of polycrystalline powder of vanadium-doped forsterite, and the growth of single crystals of vanadium-doped forsterite by the floating zone method.



**Figure 2.** UV-vis spectra of: (A)  $\text{VO}(\text{OMe})_3$  in MeOH; (B) reaction mixture of  $\text{Mg}(\text{OMe})_2$ , TEOS, and  $\text{VO}(\text{OMe})_3$  in MeOH; (C) reaction product of  $\text{VO}(\text{OMe})_3$  and  $\text{H}_2\text{O}_2$  in MeOH.

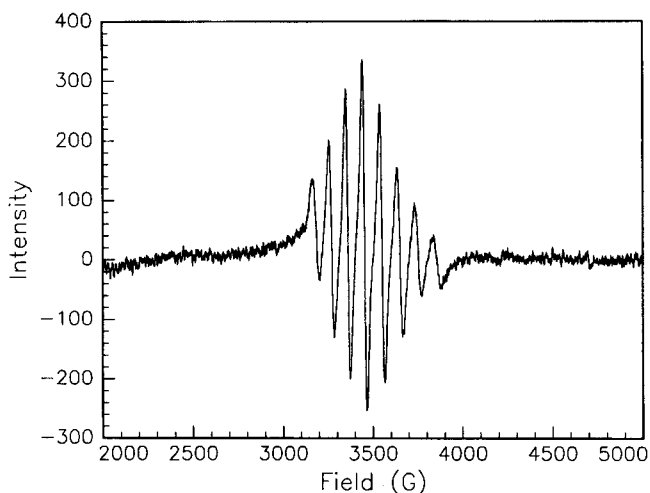


**Figure 3.** ESR spectrum obtained from the mixture of  $\text{Mg}(\text{OMe})_2$ , TEOS, and  $\text{VO}(\text{OMe})_3$  in MeOH. Eight well resolved hyperfine structures are due to  $^{51}\text{V}(I=7/2)$ .

the structure was pseudo octahedral.<sup>17</sup> It was reported that  $\text{VO}(\text{OR})_3$  ( $\text{R}=\text{OEt}$ ,  $\text{O-n-Pr}$ ,  $\text{O-n-Bu}$ ) existed as a mixture of oligomers and monomers in solution, and that the oligomeric species had square pyramidal coordination, whereas monomers had tetrahedral one.<sup>18</sup> Therefore, it was assumed that  $\text{VO}(\text{OMe})_3$  existed mostly as oligomeric species in MeOH.

Upon addition of this bluish green vanadium source solution to the clear mixture of  $\text{Mg}(\text{OMe})_2$  and TEOS, the color turned bright yellowish green instantaneously, and all the peaks were replaced by two broad peaks centered around

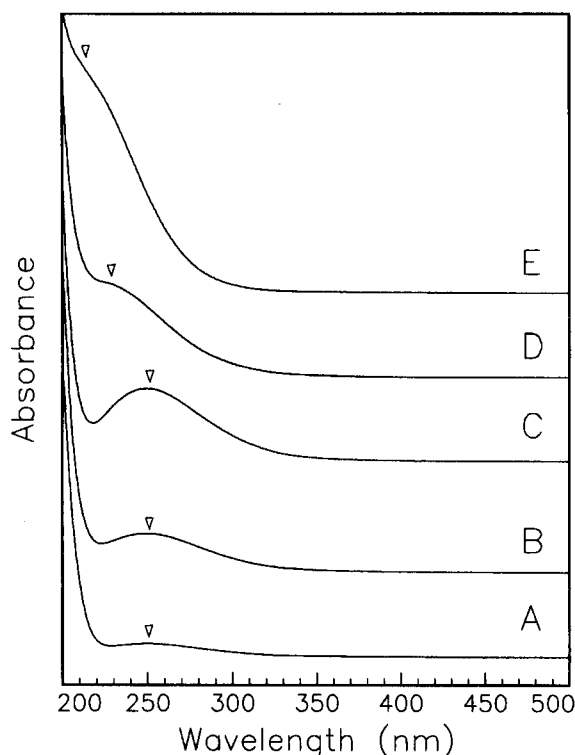


**Figure 4.** UV-vis spectra taken from the vanadium-doped forsterite sol during hydrolysis reaction. The spectra were taken after addition of methanolic 30% aqueous  $\text{H}_2\text{O}_2$ ; (A) 30 mL, (B) 60 mL, (C) 90 mL, (D) 120 mL, and (E) after all hydrolyzing reagents ( $\text{H}_2\text{O}_2$  followed by  $\text{H}_2\text{O}$ ) were added.

270, and 390 nm (Figure 2b). The ESR spectrum obtained from this reaction mixture (Figure 3) showed eight very well resolved lines, a typical hyperfine structure of  $\text{V}(\text{IV})$  due to  $^{51}\text{V}$  ( $I=7/2$ ). The isotropic spectrum indicated that the ESR active ions were in free motion.<sup>19</sup> Therefore, the immediate color change from bluish green to bright yellowish green was related to the conversion of vanadium(V) ions into vanadium(IV). At the same time, it was suggested that the oligomeric species disintegrated into monomeric ones. Three d-d transition peaks of vanadium(IV) complexes fall in the ranges 900-600, 700-500, and 500-300 nm.<sup>20</sup> But, it was not expected that those d-d transitions would be observable in this study, because d-d transition had relatively small molar extinction coefficients, and the concentration of vanadium ( $5 \times 10^{-6}$  M during measurement) was very low. For the reason, we didn't further pursue the weak d-d transition peaks.

Upon addition of  $\text{H}_2\text{O}_2$  on the reaction mixture, a broad peak developed at 255 nm (Figure 4a). As more  $\text{H}_2\text{O}_2$  was added, the intensity of the peak gradually increased, and reached a maximum when half of the  $\text{H}_2\text{O}_2$  had been added (Figure 4c). With this spectroscopic change, the color of the sol lightened significantly, and the solution became almost colorless with a light tint of yellow. The ESR spectrum of this clear sol showed no signal, indicating that vanadium(IV) had oxidized to vanadium(V). The opposite spectroscopic change was reported to be observed during aging of polyvanadic acid.<sup>21</sup> Freshly prepared acid showed a shoulder at 260 nm which was replaced by two peaks at 268 and 381 nm upon aging. ESR measurements on these two solutions

indicated that aged solution contained vanadium(IV), whereas it was absent in the freshly prepared acid. Considering the above report, it was suggested that the new peak at 255 nm with the absence of ESR signal was related to a redox transition of vanadium(IV) to vanadium(V) species. Unlike the previous redox reaction in which vanadium(V) turned to vanadium(IV) upon being mixed with a reaction mixture of  $\text{Mg}(\text{OMe})_2$  and TEOS, the initial addition of  $\text{H}_2\text{O}_2$  (when hydrolysis reaction is predominant over condensation) induced the oxidation of vanadium(IV) back to vanadium(V).

Oxidation of vanadium(IV) by dissolved air in alkaline solution was reported that the reaction proceeded through the formation of a hydrogen peroxide intermediate, which reacted with vanadium(IV) to form vanadium(V).<sup>22</sup> Adding  $\text{H}_2\text{O}_2$  directly to a methanol solution of  $\text{VO}(\text{OMe})_3$  (both in approximately the same concentration as used in the sol-gel synthesis) formed a brown solution. A spectrum taken of this reaction product had a single broad peak centered around 340 nm (Figure 2c). This peak was never observed during the sol-gel synthesis. Therefore, it appeared that the oxidation of vanadium during the initial hydrolysis was caused by some kind of oxidizing center which was different from free  $\text{H}_2\text{O}_2$ . The unusual oxidation of chromium(II) into chromium(VI) observed during the sol-gel synthesis of chromium-doped forsterite showed similar phenomena; it was observed that chromium(II) was almost instantaneously oxidized to chromium(VI) by the oxidizing moieties in the gel, when it was added after the initial hydrolysis was preceded.<sup>6</sup>  $\text{Mg-OOH}$  center was proposed to be the oxidizing center. Therefore, it was considered that the unusual redox reaction of vanadium described above added one more circumstantial evidence on the  $\text{Mg-OOH}$  intermediate. Considering the chromium(VI) remained unchanged even after the condensation reaction completed,<sup>6</sup> it could be conceived that redox reaction in vanadium was more sensitive to the rigidity of the surrounding matrix than in chromium.

The peak at 255 nm shifted toward shorter wavelength as more hydrolyzing agent was added, and reached 225 nm (sh, Figure 4e) when the addition of the hydrolyzing agents had been completed. The first charge transfer band of vanadium(IV) in  $\text{VO}(\text{acac})_2$  showed distinct red shift of about 50 nm upon oxidation,<sup>16</sup> that was postulated to be caused by a release of repulsion energy related to the oxidation of vanadium(IV) to vanadium(V). Therefore, the gradual blue shift (~30 nm) of this first charge transfer peak upon the further addition of the  $\text{H}_2\text{O}_2$  solution (now, condensation reaction should be predominant over the hydrolysis) was consistent with the reduction of vanadium(V) back to vanadium(IV) species. The ESR signal of vanadium(IV) observed from dried xerogel (Figure 5a) corroborated this reduction reaction upon further addition of  $\text{H}_2\text{O}_2$ . Whether all the vanadium would be reduced was not clear. Reduction reaction between vanadic acid (vanadium(V)) and  $\text{H}_2\text{O}_2$  in highly acidic solution was reported.<sup>23</sup> Also, it is well known that  $\text{H}_2\text{O}_2$  acts both as an oxidizing or as a reducing agent.<sup>24</sup> Therefore, the vanadium species in the reaction mixture underwent several reversible redox reactions during hydrolysis and condensation, and swung back and forth between vanadium(IV) and vanadium(V). This seesaw redox transition was summarized in Scheme 1.

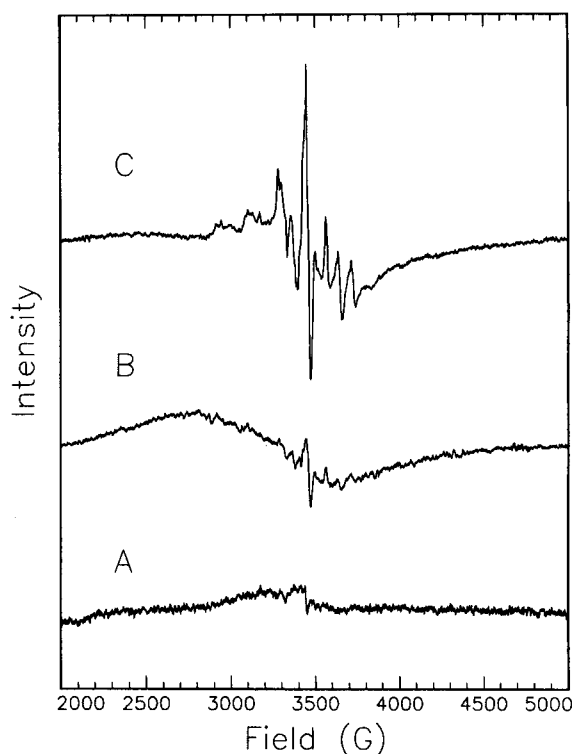
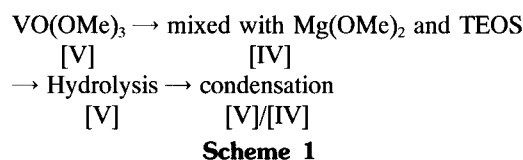


**Figure 5.** ESR spectra taken from vanadium-doped forsterite xerogel as prepared (A), polycrystalline vanadium-doped forsterite obtained by heating the xerogel at 1100 °C in air (B), and polycrystalline vanadium-doped forsterite obtained by heating the xerogel at 1100 °C in a mixture of  $\text{CO}$ ,  $\text{CO}_2$ ,  $\text{Ar}$  (1 : 5 : 10 volume ratio) (C).



The ESR spectra taken from dried xerogels showed very weak signals from vanadium(IV) ions in a rigid environment (Figure 5a). These peaks persist even after the xerogel was heated at 1100 °C in air (Figure 5b). The observation that the vanadium in its lower oxidation state was persistent even after the xerogel was heat treated in highly oxidizing atmosphere, and that the vanadium(V) in the gel reduced to vanadium(IV) during condensation indicated that the rigid environment might have encouraged the reduction of vanadium into its lower oxidation state. This reduction of vanadium in rigid environment was routinely observed during the synthesis of  $\text{V}_2\text{O}_5$  gels,<sup>25</sup> and it was well known that the  $\text{V}_2\text{O}_5$  gels were very sensitive toward reduction. When the xerogel was heated in a mixture of  $\text{CO}$ ,  $\text{CO}_2$ , and  $\text{Ar}$ , more vanadium(IV) was generated, and the ESR spectrum showed eight sharp lines with non-isotropic overall structure (Figure 5c). This non-isotropic pattern was typical of vanadium(IV) restrained in a rigid surrounding structure that was pseudo-octahedral, as in solvated  $[\text{VO}(\text{H}_2\text{O})_5]^{2+}$ ,<sup>19,26</sup>  $\text{V}_2\text{O}_5 \cdot 0.5\text{H}_2\text{O}$ ,<sup>19</sup> vanadium-doped  $\text{TiO}_2$ ,<sup>27</sup> or vanadium-doped  $\text{SnO}_2$ .<sup>28</sup>

When heated at ~1000 °C in either reducing or oxidizing

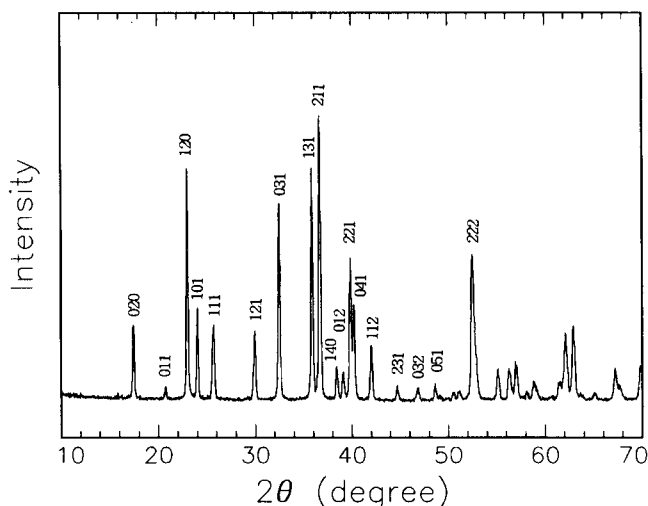


**Figure 6.** XRD pattern taken from the polycrystalline powder of vanadium-doped forsterite obtained by heating the xerogel at 1100 °C in air.

atmosphere, the vanadium-doped forsterite xerogel formed single phase forsterite, as shown by XRD pattern in figure 6. With practically no diffusion barrier, that was achieved through the homogeneity of the gel, the precursor started to become crystalline around 700 °C, and no minor phase developed during crystallization. If the material were to be synthesized by conventional solid state reaction, it would require heating at much higher temperature (above 1000°C) during much longer period (days).<sup>29</sup> The color of the polycrystalline powder was slightly yellowish when it was heated in an oxygen atmosphere, whereas it was greenish gray when heated in a reducing atmosphere.

Figure 7 showed the thermal analysis on the vanadium-doped forsterite xerogel. About 20% weight loss occurred below 550 °C. The endothermic weight loss ~100 °C was the loss of adsorbed solvent.<sup>30</sup> The exothermic weight loss ~270 °C should be attributed to the loss of bound organic groups.<sup>31</sup> Unlike the undoped or chromium-doped forsterite xerogel,<sup>8</sup> a weight loss of ~5% at 556 °C was endothermic. Instrumental cause was eliminated by repeated runs on different batches, and on pure forsterite xerogels without vanadium

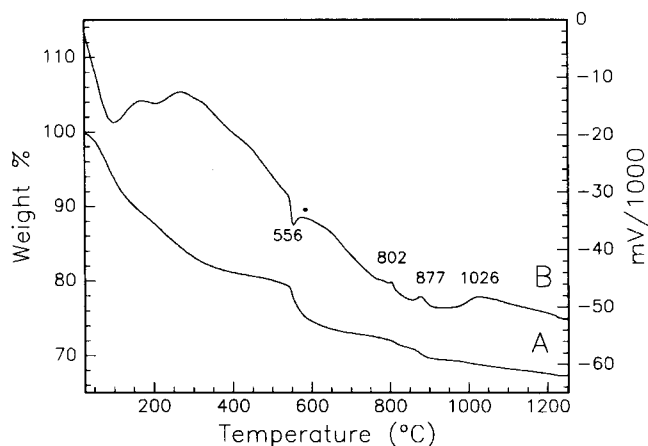
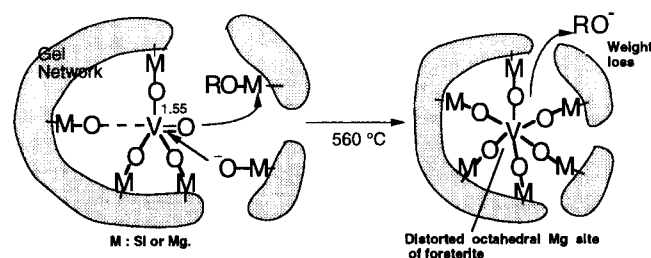


**Figure 7.** TG trace (A), and DTA curve (B) of vanadium-doped forsterite xerogel. The xerogel was heated in dry oxygen (200 mL/min) at a rate of 10°C/min.

in it, which registered an exotherm for thermal decomposition of the organic residues. The endotherm could not be attributed to decomposition of an organic ligand. Decomposition of organic ligands, accompanying CO<sub>2</sub> generation, should have registered an exotherm around 570°C.<sup>8</sup> It is known that vanadium compounds have a very short bond in multiple-bond character, that results in a [VO<sub>5</sub>] environment with a very short V=O double bond.<sup>32</sup> Especially when the vanadium is in its oxidation state of IV, the V=O bond is very strong, and even suggested to have partial triple bond character.<sup>33</sup> Also, V=O in double bond character is known to be stable in silica supported vanadium complexes.<sup>34</sup> It was suggested that vanadium oxide bonds with multiple character might transform into single bonds around 550°C, which could cause endothermic heat event. The concomitant weight loss of around 4% indicated that organic residues were expelled without being pyrolyzed during the transformation. Possible route of this endothermic process was suggested in the Scheme 2 where the bond length<sup>33,35</sup> and local structures<sup>33,35,36</sup> were presumed on the bases of the precedent results. The process involved the exclusion of unhydrolyzed alkoxy groups, which corresponded to the weight loss observed by TGA. The existence of the remaining alkoxy groups at such high temperature, prior to the endothermic exclusion, had already been proved in previous study.<sup>7</sup>

The exothermic heat events at 802 and 877 °C corresponded to the crystallization of the crystalline intermediate phase and forsterite, respectively.<sup>7</sup> Both crystallization accompanied 1-2% weight losses, as was observed for chromium-doped forsterite xerogel. A very broad exothermic weight loss ~1020 °C was speculated to be the loss of residual OH groups. This exothermic weight loss of 1-3% has been commonly observed between 1100 and 1250 °C for forsterite and metal-doped forsterite xerogels synthesized by the H<sub>2</sub>O<sub>2</sub>-assisted sol-gel method.

Single crystals of vanadium-doped forsterite were grown both in a reducing or oxidizing atmosphere by the floating zone method, by using the feeding rods made from the polycrystalline vanadium-doped forsterite powder. Unlike chromium-doped forsterite, which generated vaporized chromium oxide (CrO<sub>2</sub>) during single crystal growth, no volatile was generated during melting of the vanadium-doped forsterite. The concentration of vanadium, analyzed by microprobe and ICP/MS, was shown in Table 1. More than 90% of vanadium was lost during melting, even though apparently no volatile byproduct was observed during single crystal growth. Judging by the dark coloration of the tip of the melt, the partitioning of vanadium to liquid phase was greater than that in solid phase. Thereby, only a small fraction of vanadium added to the polycrystalline powder (feeding stock)



**Scheme 2**

**Table 1.** Dopant level in the single crystals of vanadium-doped forsterite. The analyses were carried out by microprobe (WDS) and ICP/MS

| atmosphere for crystal growth | level in xerogel | level in crystal (ppm) | dopant loss (%) |
|-------------------------------|------------------|------------------------|-----------------|
| reducing                      | 3608             | 265                    | 93              |
| oxidizing                     | 3608             | 145                    | 96              |
| oxidizing                     | 362              | 27                     | 93              |

was doped in the single crystal, while rest of it remained in the melt. Therefore, in order to dope certain amount of vanadium into a single crystal, one should dope the feeding stock with excess amount of vanadium. As far as this study suggested, the dopant concentration in the feeding stock should be ten times more than that in the single crystal. With this high content of vanadium, the feeding stock made from a simple mixture of constituent metal oxides would surely form minor phases, which render the crystal growth by the floating zone method impossible.

The crystals grown in a reducing atmosphere had a greenish blue color and the ones grown in an oxidizing atmosphere were pale blue. Unlike the chromium-doped forsterite that showed strong pleochroism,<sup>14</sup> the vanadium-doped forsterite showed similar absorption patterns and color through three orthogonal unit cell axes. The spectrum appeared to be combination of three major absorptions at 700, 825, and 1075 nm. The peak at 700 nm was shown to differ from

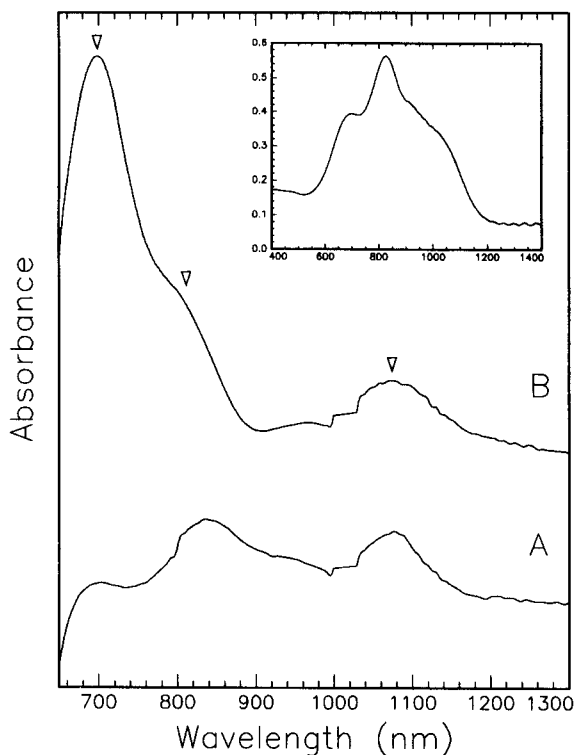


**Figure 8.** The absorption spectra taken from a single crystal of vanadium-doped forsterite. The crystal was grown in pure oxygen by the floating zone method. The step around 1000 nm was caused by an instrumental artifact. The beam was polarized so that (A) E//b, or (B) E//c. The inset shows the absorption spectrum of the single crystal grown in reducing atmosphere, observed through a-axis.

the other two peaks.

The spectra in Figure 8 showed the absorption spectra through different polarization for the crystal grown in an oxidizing atmosphere. The peak at 700 nm shows very different absorptivity from a set of the other two peaks at 825 and 1075 nm, upon polarization along two different directions. The absorbance of the 700 nm peak at E//c was much greater than that at E//b. An absorption spectrum taken of the crystal grown in a reducing atmosphere along the a-axis was shown in the inset of the Figure 8. Although the overall features of the spectra are similar, the absorbance of the crystal grown in an oxidizing atmosphere was significantly lower than that of the crystal grown in a reducing atmosphere, indicating the color center was vanadium(IV). By assessing the absorption, the vanadium color center in forsterite was considered to have proper absorption for the crystal to be excited by available lasers. Although the vanadium-doped forsterite single crystal had proper absorption characteristics to be excited by Nd:YAG laser, it did not have any emission in near infra-red range, the range in which we were interested to look at.

## Conclusion

Forsterite which was doped with vanadium was synthesized as a single phase polycrystalline powder via the H<sub>2</sub>O<sub>2</sub>-assisted sol-gel method. The VO(OMe)<sub>3</sub> dissolved in methanol was suggested to be oligomeric in oxidation state V. Upon being mixed with the reaction mixture of Mg(OMe)<sub>2</sub> and TEOS, the oligomeric species apparently disintegrated into monomeric ones, and the vanadium(V) reduced to vanadium(IV). During the initial hydrolysis reaction, the vanadium(IV) oxidized back to vanadium(V), which corroborated the formation of highly oxidizing moieties (possibly Mg-OOH) in the gel during initial hydrolysis step. As the condensation reaction set in, apparently the vanadium(V) (probably not all) reduced back to vanadium(IV). Vanadium-doped forsterite powder contained vanadium(IV) even when it was calcined in highly oxidizing atmosphere.

By using the polycrystalline powder as a feeding stock, single crystals of vanadium-doped forsterite were grown by the floating zone method both in highly oxidizing or in reducing atmosphere. The partition of vanadium in molten liquid phase was so high that only a small fraction (less than 10%) of the vanadium in the polycrystalline powder remained in the single crystals. The color center of the crystal was vanadium(IV). The absorption was observed at 700, 825, and 1075 nm, and no emission was observed in near infra-red range.

**Acknowledgment.** This work was supported by the MRL program of NSF. Support by the Ministry of Education (BSRI-96-3404) was acknowledged with gratitude. Authors thank to Duane B. Barber and Professor Clifford R. Pollock, for their contribution to the measurements of absorption spectra.

## References

1. Deer, W. A.; Howie, R. A.; Zussman, J. *Rock-Forming Minerals Vol 1A, Orthosilicates*; Halsted: New York, 1982; p 1.

2. Petricevic, V.; Gayen, S. K.; Alfano, R. R.; Yamagishi, K.; Anazai, H.; Yamaguchi, Y. *Appl. Phys. Lett.* **1988**, *52*, 1040.
3. Budil, D. E.; Park, D. G.; Burlitch, J. M.; Geray, R. F.; Diekmann, R.; Freed, J. H. *J. Chem. Phys.* **1994**, *101*(5), 3538.
4. Maiman, T. H.; Hoskins, R. H.; D'Haenens, I. T.; Asawa, C. K.; Evtuhov, V. *Phys. Rev.* **1961**, *123*, 1151.
5. Walling, J. C.; Peterson, O. G.; Jenssen, H. P.; Morris, R. C.; O'dell, E. W. *IEEE J. Quantum Elect.* **1980**, *QE-16*(12), 1302.
6. Park, D. G.; Burlitch, J. M.; Geray, R. F.; Dieckmann, R.; Barber, D. B.; Pollock, C. R. *Chem. Mater.* **1993**, *5*, 518.
7. Park, D. G.; Duchamp, J. C.; Burlitch, J. M.; Duncan, T. M. *Chem. Mater.* **1994**, *6*(11), 1990.
8. Park, D. G.; Martin, M. H. E.; Ober, C. K.; Burlitch, J. M.; Cavin, O. B.; Porter, W. D.; Hubbard, C. R. *J. Am. Ceramic Soc.* **1994**, *77*(1), 33.
9. Yeager, K. E.; Burlitch, J. M. *J. Non-Cryst. Solids* **1992**, *149*, 179.
10. Yeager, K. E.; Burlitch, J. M.; Loehr, T. M. *Chem. Mater.* **1993**, *5*, 525.
11. Burlitch, J. M. *How to Use Ace No-Air Glassware-Bulletin 3840*; Ace Glass Co. Inc.: Vineland NJ, 1984; p 1.
12. Charles, N. C.; Smith, H. M.; Watenpugh, K. *Inorg. Chem.* **1966**, *5*, 2131.
13. Hosoya, S.; Takei, H. *J. Crystal Growth* **1982**, *57*, 343.
14. Higuchi, M.; Geray, R. F.; Dieckmann, R.; Park, D. G.; Burlitch, J. M.; Barber, D. B.; Pollock, C. R. *J. Crystal Growth*, **1995**, *148*, 140.
15. Clark, R. J. H. *Comprehensive Inorganic Chemistry*; Bailar, J. C.; Emeleus, H. J.; Nyholm, R.; Trotman-Dickenson, A. F. Ed.; Pergamon Press: New York, 1973; p 509.
16. Ortolano, T. R.; Selbin, J.; McGlynn, S. P. *J. Chem. Phys.* **1964**, *41*, 262.
17. Dodge, R. P.; Templeton, D. H.; Zalkin, A. *J. Chem. Phys.* **1961**, *35*, 55.
18. Sanchez, C.; Nabavi, M.; Taulelle, F. *Better Ceramics Through Chemistry III. Mater. Res. Soc. Symp. Proc.* **1988**, *121*, 93.
19. Livage, J. *Chem. Mater.* **1991**, *3*, 578.
20. Selbin, J. *Chemical Reviews* **1965**, *65*, 153.
21. Lemerle, J.; Nejem, L.; Lefebvre, J. *J. Inorg. Nucl. Chem.* **1980**, *42*, 17.
22. Dean, G. A.; Herringshaw, J. F. *Talanta* **1963**, *10*, 793.
23. Cain, J. R.; Hostetter, J. C. *J. Am. Chem. Soc.* **1912**, *34*, 274.
24. Greenwood, N. N.; Earnshaw, A. *Chemistry of Elements*; Oxford, 1984; p 745.
25. Gharbi, N.; Sanchez, C.; Livage, J.; Lemerle, J.; Nejem, L.; Lefebvre, J. *Inorg. Chem.* **1982**, *21*, 2758.
26. Ballhausen, C. J.; Gray, H. B. *Inorg. Chem.* **1962**, *1*, 111.
27. Gerritsen, H. J.; Lewis, H. R. *Phys. Rev.* **1960**, *119*, 1010.
28. Kasai, P. H. *Phys. Lett.* **1963**, *7*, 5.
29. Borchardt, V. G.; Schmalzried, H. *Ber. Dtsch. Keram. Ges.* **1972**, *49*, 395.
30. Orgaz, F.; Rawson, H. *J. Non-Cryst. Solids* **1986**, *82*, 57.
31. Brinker, C. J.; Haaland, D. M. *J. Am. Ceram. Soc.* **1983**, *66*, 758.
32. Nabavi, M.; Taulelle, F.; Sanchez, C.; Verdaguer, M. *J. Phys. Chem. Solids* **1990**, *51*, 1375.
33. Cotton, F. A.; Wilkinson, G. *Advanced Inorganic Chemistry, 5th Ed.*; John Wiley & Sons: 1988; p 672.
34. Feher, F. J.; Walzer, J. F. *Inorg. Chem.* **1991**, *30*, 1689.
35. Clark, R. J. H. *Vanadium; in Comprehensive Inorganic Chemistry*; Pergamon Press: 1973; p 513.
36. Birle, J. D.; Gibbs, G. V.; Moore, P. B.; Smith, J. V., *Am. Miner.* **1968**, *53*, 807.